Research paper

Solvent-free Temperature-Facilitated Direct Extrusion 3D Printing for Pharmaceuticals

Magda Kuźmińska[1,2], Beatriz Pereira[1], Rober Habashy[1], Matthew Peak[3], Mohammad Isreb[4], Tim D Gough[5], Abdullah Isreb[1,*], Mohamed A Alhnan[6,**]

[1]*School of Pharmacy and Biomedical Sciences, University of Central Lancashire, Preston, Lancashire, UK*

[2] *School of Pharmacy and Biomedical Sciences, University of Central Lancashire, Preston, Lancashire, UK; Faculty of Pharmacy with the Laboratory Medicine Division, Medical University of Warsaw, Warsaw, Poland*

[3]*Paediatric Medicines Research Unit, Alder Hey Children's NHS Foundation Trust, Liverpool, UK*

[4]*School of Pharmacy and Medical Sciences. University of Bradford UK*

[5]*Centre for Pharmaceutical Engineering Sciences, University of Bradford UK*

[6]*Institute of Pharmaceutical Sciences, King's College London, London, UK*

*Corresponding author:
Dr Abdullah Isreb
School of Pharmacy and Biomedical Sciences.
MB141 Maudland Building
University of Central Lancashire, Preston.
PR1 2HE
Lancashire
Email: AIsreb@uclan.ac.uk

**Corresponding author:
Dr Mohamed A Alhnan
Institute of Pharmaceutical Sciences
King's College London
150 Stamford Street
London SE1 9NH. Tel.: +44 (0)20 7848 7265.
Email: Alhnan@kcl.ac.uk

Abstract

In an era moving towards digital health, 3D printing has successfully proven its applicability in providing personalized medicine through a technology-based approach. Among the different 3D printing techniques, semisolid extrusion 3D printing has been demonstrated as a promising approach for on demand manufacturing of solid dosage forms. However, it usually requires the use of elevated temperatures and/or the incorporation of an evaporable solvent (usually water). This can implicate the addition of drying step, which may compromise the integrity of moisture- or temperature-sensitive drugs, and open the door for additional quality control challenges,

Here, we demonstrate a new approach that simplifies semisolid extrusion 3D printing process with the elimination of the post-printing drying step, by merely adding a fatty glyceride, glyceryl monostearate (GMS), to a model drug (theophylline) and permeable water insoluble methacrylate polymers (Eudragit RL and RS). Indeed, rheological studies indicated that the addition of a combination of a plasticiser, triethyl citrate, and GMS to theophylline: methacrylate polymer blend significantly reduced the extensional viscosity (to < 2.5 kPa.Sec) at 90 ^{o}C. Interestingly, GMS demonstrated a dual temperature-dependant behavior by acting both as a plasticizer and a lubricant at printing temperature (90-110 °C), while aiding solidification at room temperature. X-ray powder diffraction indicated incomplete miscibility of GMS within the polymeric matrix at room temperature with the presence of a subtle diffraction peak, at 2(Θ)= 20. The 3D printed tablets showed acceptable compendial weight and content uniformity as well as mechanical resistance. *In vitro* theophylline release from 3D printed tablets was dependant on Eudragit RL:RS ratio.

All in all, this work contributes to the efforts of developing a simplified, facile and low-cost 3D printing for small batch manufacturing of bespoke tablets that circumvents the use of high temperature and post-manufacturing drying step.

Keywords: Direct ink writing; Early phase clinical trials; Material extrusion; Patient-specific; Personalized; Small batch.

1. Introduction

The increasing trend towards individualised medicine in healthcare has led to exploring the potential of several 3D printing techniques as an on-demand manufacturing tool of solid dosage forms (Alhnan et al., 2016; Pravin and Sudhir, 2018). Among these, fused deposition modelling (FDM) 3D printing has been an extensively researched approach owing to its low cost, lack of drying and/or finishing steps and dependence on an established technique of Hot Melt Extrusion (HME) for producing filaments (Alhijjaj et al., 2019; Melocchi et al., 2016; Skowyra et al., 2015). Several modifications have been attempted to reduce the thermal stress associated with this technology through the use of plasticizers (Okwuosa et al., 2016; Pereira et al., 2019) and low melting/glass transition temperature polymers (Kollamaram et al., 2018). However, the requirement for fabrication of drug-loaded filaments for FDM 3D printing has led to interest in simplification of the fabrication process to shorten the thermal exposure of the active pharmaceutical ingredient(s) and excipients.

Semi-solid extrusion is a 3D printing technology that consists of extrusion of semi-solid materials such as pastes (Cui et al., 2020; Khaled et al., 2014) and gels (Tagami et al., 2019) through a defined size nozzle to create a new structure after solidification (e.g. tablets). The use of a such technique eliminates the need for an intermediate step of filament manufacturing prior to 3D printing. Semi-solid extrusion has been previously used to demonstrate the feasibility of producing multi-drug solid dosage forms with individualised drug-release profile (Khaled et al., 2015a; Khaled et al., 2015b). Later, the same technology was demonstrated to manufacture gastro-floating tablets (Li et al., 2018), dose-flexible systems with immediate-release profile (Cui et al., 2019), and orodispersible films (Yan et al., 2020). In addition, it avoids a high processing temperature, thus poses an attractive alternative to FDM. However, the starting materials and their mixing ratios should be carefully considered to meet the required strict rheological properties that allows a smooth, reproducible and efficient extrusion which can solidify following 3D printing completion (Cheng et al., 2020; Yang et al., 2020). In most cases, solvent (often water) is used to facilitate material flow through increasing the plasticity of the extrudate (Khaled et al., 2018). However, this approach opens the door to two challenges; the inclusion of an additional drying step for the printed product, along with quality control and logistic issues associated

with it, and the risk of drug degradation mainly due to hydrolysis. More recently, we have reported a hybrid approach of combining both solvent and temperature to produce immediate and extended release tablets at a relatively moderate temperature range (Dores et al., 2020).

Therefore, a more simplified process that avoids a post-printing process is needed. Recently, hydroxypropyl cellulose (HPC)-based tablets with immediate (Fanous et al., 2020) and sustained release profiles (Goyanes et al., 2019) were produced by using an elevated temperature and shear forces using pneumatic or screw-based extrusion. An alternative solution was the use of a low melting carrier (e.g. PEG4000, melting point of approximately 65 °C) to fabricate immediate-release tablets (Li et al., 2019).

Eudragit® RL and RS are insoluble poly(meth)acrylates with pH-independent swelling with high and low water permeabilities, respectively (Evonik). These have been widely used in combination for customisation of drug release profile (Duarte et al., 2007), including using FDM 3D printing (Krause et al., 2019; Pietrzak et al., 2015). In this work, we report the use of semi-solid extrusion as a single 3D printing step. The novel use of a fatty glyceride (glycerol monostearate) as both a lubricant and a solidifying agent was also demonstrated. GMS is a poorly water soluble excipient used in food, cosmetic and pharmaceutical applications for its emollient, emulsifier and plasticiser properties (Rowe, 2009). In solid dosage forms, it is usually added as a lubricant (Zhu et al., 2004) or a sustained-release matrix (Laila et al., 2009; Peh et al., 2000; Peri et al., 1994).

2. Materials and methods

2.1 Materials

Theophylline was obtained from Acros Organics (UK). Eudragit® RL100 and RS100 were donated by Evonik (Darmstadt, Germany). Triethyl citrate (TEC) was obtained from Sigma-Aldrich (Dorset, UK). Glyceryl monostearate (GMS) (Imwittor K900) was a donation from Oleo GmbH (Germany).

2.2 Hansen Solubility Parameters (HSP) calculations

Functional group contribution method was used to calculate the HSP values of the API and excipients. HSPiP software (version 5.3.03) was used to calculate the δD (Dispersion component), δP

(Polar component, δH (Hydrogen-bonding component) and δT (Total) using the canonical SMILE of each compound.

2.3 Rheological Studies

Extensional rheology, measured by capillary rheometer, was selected for screening ingredients and initial formulations due to its similarity to syringe extrusion. Advanced Capillary Rheometer RH10 (Bohlin Instruments, UK) was used to assess the extensional viscosity of the mixtures presented in **Table I**. The samples were fed into the two barrels of the rheometer each fitted with a 1mm diameter die at 90^{o} angle (one long die (16 mm) and one orifice die (0mm)). The barrel was heated to 90°C for 10 min before the experiment started. The formulations were subjected to two precompression stages at 0.5 and1MPa. The test was carried out at a shearing rate of 20, 50, 100 Sec^{-1}. The twin barrels allow simultaneous measurement of both shear flow and entry pressure by comparing the pressure difference between the long and orifice dies. The extensional was calculated using Hagen–Poiseuille equation (Coates et al., 1998):

$$\Delta p = \frac{8\mu LQ}{\pi r^4}$$

where Δp is the pressure difference between the long and orifice dies, L is the length of die, μ is the extensional viscosity, Q is the volumetric flow rate, r is the radius of die.

2.4 Preparation of the feed for semi solid extrusion

The prepared formulations with the required mixing ratios of materials are highlighted in **Table II**. The methacrylate polymer(s) (Eudragit RL and RS), GMS and theophylline were accurately weighed and mixed using a mortar and pestle. The blends were then transferred to a Krups F20342 grinder (Germany) where it was shear-mixed with TEC. Blends (approximately 10 g) were filled in a 12 mm diameter metal syringe (Hyrel 3D, Atlanta, USA) to be printed as described in Section 2.5.

2.5 Tablet design and 3D printing

Cylindrical shaped tablets (diameter: 13 mm, height: 3 mm) were designed using Autodesk® 3ds Max Design 2019 (Autodesk, Inc., USA). The designs were imported to the Slic3r (version 1.3) software in stereolithographic (STL) format. The latter were then converted to g-code files

using the following settings: first layer thickness: 0.6 mm, layer thickness: 0.3 mm, speed perimeters: 50%, infill speed: 8 mm/sec, first layer build speed: 6 mm/sec and travel speed: 15 mm/sec. The nozzle and filament diameters were set as 1.194 mm.

A Hyrel System 30M (Hyrel 3D, Atlanta, USA) equipped with a VOL-25 (Volcano) modular head and a 16-gauge stainless steel tip was used to manufacture the tablets. The standard glass plate was covered with an acrylic sheet to achieve a better adhesion of the printed layers to the base plate. The following settings were used for the Repetrel software (version 3.0) for the printer head: infill percentage: 100%, Z-layer thickness: 0.3, motor pulses rate: 2.3 pulses/nL and a material flow multiplier of 0.8 mm. Prior to 3D printing, the syringe body was placed in an aluminium heated sleeve/housing where the feed was heated for 30 min.

2.6 Thermal analysis

Raw materials and samples of the 3D printed tablets were analysed by:

a) Thermogravimetric analysis (TGA) Samples of approximately 10 mg were scanned in triplicate in platinum pans using a TGA Q500 (TA Instruments, Elstree, Hertfordshire, UK). Samples were heated at a rate of 10°C/min from 25°C to 500°C with a nitrogen purge of 40:60 mL/min for furnace: sample, respectively. b) Differential scanning calorimetry (DSC): Samples (~5 mg) were scanned in triplicate in standard aluminium pans at a heating rate of 10°C/min from -50 to 300 °C, with a nitrogen purge of 50 mL/min, using a DSC Q2000 (TA Instruments, Elstree, UK). TA Universal analysis software (v 4.5A, TA Instruments, Elstree, UK) was used to analyse data for both TGA and DSC.

2.7 X-Ray Powder Diffractometry (XRPD)

The physical form of the drug and excipients within the 3D printed tablets was assessed using a powder X-ray diffractometer, D2 Phaser with Lynxeye (Bruker, Germany). Samples were scanned from 2Theta = 5° to 50° using a 1.25 s time count and 0.01° step width. The divergence slit was 1 mm and the scatter slit was 0.6 mm. The filament emission was 10 mA with a scan type coupled with a theta/theta scintillation counter over 60 min. A voltage of 30 kV was used, the wavelength was 0.154 nm using Cu source and a voltage of 30 kV.

2.8 Characterization of the 3D printed tablets

The mechanical properties of the 3D printed tablets were assessed by measuring tablet hardness using an Agilent 200 Tablet Hardness Tester (Agilent Technologies, Germany). The test was done in triplicate. The friability of 3D printed tablets was assessed by accurately weighing tablets (n=10), which were then placed in the apparatus drum of Agilent Dual-drum Friability Tester 250 (Agilent Technologies), and rotated 100 times.

A digital calliper (eSYNic, China) was used to measure the radius and the thickness of the tablets (n=10). The weight uniformity of the 3D printed tablets was determined by weighing approximately 10 tablets randomly selected from each preparation. The average mass, standard deviation and percentage deviation from average mass were determined for each batch.

2.9 Analysis of drug content using HPLC

The drug content of the 3D printed tablets was assessed using an Agilent 1260 series UV-HPLC (Agilent Technologies, Germany) with XTerra RP 18 column (150 × 4.6 mm, 5 μm particle size) (Waters, Ireland) as previously described (Okwuosa et al., 2016). The injection volume was 5 μL and the mobile phase used consisted of 10 mM ammonium acetate buffer: methanol: acetonitrile (86:7:7). The analysis was carried out at a flow rate of 1 mL/min, at 40°C, with a run time of 7 min and wavelength of 272 nm.

2.10 Scanning Electron Microscopy (SEM)

The morphology of the external and cross-sectional surfaces of the 3D printed tablets was assessed using a JCM-6000 plus NeoScope™ microscope (Jeol, Tokyo, Japan) at 10 kV. All samples were gold coated prior to imaging using a JFC-1200 Fine Coater (Jeol, Tokyo, Japan). The images were collected using Image J software (v 1.2.0., Tokyo, Japan).

2.11 In vitro dissolution

The impact of the ratio of the polymers used on the release profile of theophylline was assessed using a USP II dissolution test paddle apparatus (Erweka GmbH, Germany). Each experiment was carried out in triplicate at 37 ± 0.5°C with a rotating paddle speed of 50 rpm. The tablets were tested in 750 mL of 0.1 M HCl (pH 1.2) for 2 hrs, followed by 4 hrs exposure to pH 6.8 phosphate buffer (through the addition of 250 mL of tribasic phosphate solution 0.215 M). Data were collected each 5 min by an

UV/VIS spectrophotometer (PG Instruments Limited, UK) at a wavelength of 272 nm and a path length of 1 mm. Data were analysed using IDISis software version 2012 (Automated Lab, Berkshire, UK).

2.12 Statistical analysis

One-way ANOVA was employed using SPSS Software (22.0.0.2) to analyse the results. Differences in results less than probability level ($p < 0.05$) were considered significant.

4. Results and discussion

A schematic diagram of the developed 3D printing process can be found in **Fig. 1**. In this process, a polymer-based pharmaceutical ink is loaded to a syringe cartridge at a set temperature. In a clinical setting, the ink can be loaded as compressed powder into a cylindric shape with the dimensions of the syringe (12 mm diameter x 60 mm height). Alternatively, a single-use syringes could be used instead to avoid any cleaning step and cross-contamination between formulations.

Initial screening of compatibility using Hansen solubility parameters indicates a potential for good miscibility between the polymer, plasticiser (TEC) and GMS ($\delta T<7$ $MPa^{½}$) (**Table III**).

The shear and extensional viscosity of the polymer and various formulations were measured using an extensional rheometer. The shear viscosity of Eudragit RL (as a model polymer) confirmed its highly elastic nature even when the temperature was elevated to 110°C (**Fig. 2A**). In fact, the diameter difference between the extruded polymer from the long and orifice dies due to die swelling was significant (3.5mm vs 5 mm) (**Fig. 3A**). The extensional viscosity of the formulations detailed in **Table I** are presented in **Fig. 2B**. Plasticizing Eudragit RL with TEC reduced the polymer extensional viscosity to <3 kPa.Sec. This yielded a heavily plasticized matrix that lacked structural rigidity and was deemed unsuitable for 3D printing. On the other hand, the incorporation of GMS into Eudragit RL also maintained extensional viscosity <10 kPa.Sec at 90 ^{o}C while producing a relatively harder polymer matrix at room temperature compared to TEC. **Fig. 2B** also illustrates that adding increasing concentrations of theophylline (20 and 43%w/w) resulted in higher extensional viscosity values. It is possible that the insoluble theophylline crystals acted as a solid filling agent adding more elasticity to the formulation (Faitel'son and Alekseenko, 1977). This resulted in a highly viscous semi-solid dispersion that could not be extruded at 90^{o}C, when applied to the printer. Overall, combining TEC and GMS with theophylline: polymer blend produced the lowest viscosity (< 2.5 kPa.Sec) (**Fig. 2B**). The blend proved to be printable at 90^{o}C and yielded a quickly solidifying tablets at room temperature. In fact, the extruded filaments have a significantly less die swelling compared to the pure polymer (**Fig. 3B**), hence confirming a more desirable plasticity.

The above rheological behavior of the initial polymer blend was confirmed in the initial 3D printing trials. By using Eudragit RL or its blend with theophylline, no material could be extruded through the syringe. However, adding excess amount of plasticizer (TEC) allowed a facile flow of materials, yet it yielded highly flexible matrices with a collapsed structure that was unsuitable for 3D printing. The use of such combination (TEC and GMS) has been previously reported to facilitate HME of an Eudragit RS PO-based formulation (Zhu et al., 2004). With a melting point at 58-65 °C (Choi et al., 2016; Qushawy et al., 2019), GMS can be liquified at relatively low 3D printing temperature range (90-110 °C), which facilitates extrusion through lubricant effect, and contribute to the rapid solidification of the 3D printed structure at room temperature without the need for a post-printing drying step.

TGA was performed to assess the stability of the raw materials at the printing temperatures (90-110 °C). Eudragit RL and TEC showed 2 % of weight loss up to 110 °C (**Fig. 4**), which is believed to be due to moisture evaporation (Okwuosa et al., 2016; Pietrzak et al., 2015)**.** All components were stable at the 3D printing temperatures, confirming their suitability for the developed method. DSC thermographs of the 3D printed tablets showed an endotherm event at approximately 53-55 °C (**Fig. 4**), which is believed to be the depressed melting of GMS, indicating the presence of a portion of this component in a crystalline form. Therefore, a printing temperature above 55 °C was deemed necessary to liquidate GMS crystals and allow successful 3D printing the formulation.

Following extrusion from the nozzle, the solidification of these matrices will then provide a stable polymeric layer that can withstand the weight of subsequent stacking layers. The melting point of theophylline was observed at 272.8 ^{o}C for the pure drug. However, it was difficult to detect in the 3D printed tablets due to thermal degradation of the excipients prior to this temperature.

The XRPD pattern of the 3D printed tablets revealed diffraction peaks distinctive of theophylline at 2(Θ)= 7°, 12°, 14° and 24° (**Fig. 6**), indicating the presence of the drug in crystalline form. A subtle peak, which is believed to be characteristic of GMS, can be seen at 2(Θ)= 20 ° (**Fig. 6**). This may indicate incomplete dissolution of GMS and the presence of crystals of this component within the polymeric matrix.

SEM images of the 3D printed showed a smooth glossy surface, similar to GMS-based films(Farrell, 2010; Rajsharad, 2005), which can be explained by its lubricant characteristics. The tablets showed uniform layers (300 μm) and in general, the cross-section images showed fusion between the layers (**Fig. 7**) The 3D printed tablets demonstrated friability properties pharmaceutically acceptable (<1%) (FDA, 2017) and a high resistance to crushing force values that were not significantly different between formulations ($p>0.05$) (**Table IV**). The process also exhibited a high level of reproducibility as shown in the low variation in both tablets weight and drug contents.

Customizing theophylline release profile was achieved by manipulating the methacrylate polymer ratios: Eudragit RL: RS ratio **(Fig. 8**). Increasing content of Eudragit RS led to further delay of theophylline release from the matrix structure. This can be explained by the lower number of quaternary ammonium groups of Eudragit RS when compared with Eudragit RL (Lehmann, 1986). These groups provide higher hydrophilicity, promoting more intense interaction within the polymeric matrix, explaining the higher permeability of the polymer (Jelvehgari and Montazam, 2012; Siepmann et al., 2008).

The mechanism of drug release from Eudragit RL and RS-based drug delivery systems has been proposed to take place through the control of fluid permeation and consequent dissolution and diffusion of the drug (Glaessl et al., 2010; Steward et al., 1995). It has been shown that drug diffusion is pH independent, which can be explained by the ionization of the quaternary ammonium groups of the polymers at all pH levels with the gastrointestinal tract. On the other hand, it is dependent on its size and steric effects (Lehmann, 1997), ionic strength and the buffer used in the dissolution medium (Bodmeier et al., 1996; Wagner and McGinity, 2002).

Although the developed pharmaceutical ink proved to be highly efficient in providing a solution in avoiding pre- and post-printing processes, it is limited to extended-release dosage forms. Further advancement of the system is necessary to adapt it to immediate- and delayed release carriers.

4. Conclusions

The presented approach provides a significant advancement for semi-solid extrusion. Rather than starting with aqueous semi-solids that risks API hydrolysis, the system enables a solvent-free direct ink writing at moderate temperature range (90-110 ^{o}C) with readily-available tablet without the need for finishing or drying steps. An important inventive step is the incorporation of fatty glyceride, which demonstrated a dual temperature-dependant behavior by acting as a plasticizer and a lubricant at printing temperature while aiding solidification at room temperature. The system proved compatible with widely-used methacrylate polymers, where modulation of the release profile of the model drug could be achieve by manipulating polymer permeability species.

Alhijjaj, M., Nasereddin, J., Belton, P., Qi, S., 2019. Impact of Processing Parameters on the Quality of Pharmaceutical Solid Dosage Forms Produced by Fused Deposition Modeling (FDM). Pharmaceutics 11.
Alhnan, M.A., Okwuosa, T.C., Sadia, M., Wan, K.W., Ahmed, W., Arafat, B., 2016. Emergence of 3D Printed Dosage Forms: Opportunities and Challenges. Pharm Res 33, 1817-1832.
Bodmeier, R., Guo, X., Sarabia, R.E., Skultety, P.F., 1996. The influence of buffer species and strength on diltiazem HCl release from beads coated with the aqueous cationic polymer dispersions, Eudragit RS, RL 30D. Pharm Res 13, 52-56.
Cheng, Y., Qin, H., Acevedo, N., Shi, X., 2020. Development of methylcellulose-based sustained-release dosage by semisolid extrusion additive manufacturing in drug delivery system. Journal of Biomedical Materials Research Part B: Applied Biomaterials.
Choi, K.-O., Choe, J., Suh, S., Ko, S., 2016. Positively Charged Nanostructured Lipid Carriers and Their Effect on the Dissolution of Poorly Soluble Drugs. Molecules 21, 672.
Coates, P., Kelly, A.L., Rose, R.M., Woodhead, M., 1998. In-process Shear Flow Measurements in Extrusion and Injection Moulding
Bradford University.
Cui, M., Li, Y., Wang, S., Chai, Y., Lou, J., Chen, F., Li, Q., Pan, W., Ding, P., 2019. Exploration and Preparation of a Dose-Flexible Regulation System for Levetiracetam Tablets via Novel Semi-Solid Extrusion Three-Dimensional Printing. Journal of Pharmaceutical Sciences 108, 977-986.
Cui, M., Pan, H., Fang, D., Qiao, S., Wang, S., Pan, W., 2020. Fabrication of high drug loading levetiracetam tablets using semi-solid extrusion 3D printing. Journal of Drug Delivery Science and Technology 57, 101683.
Dores, F., Kuźmińska, M., Soares, C., Bohus, M., A Shervington, L., Habashy, R., Pereira, B.C., Peak, M., Isreb, A., Alhnan, M.A., 2020. Temperature and solvent facilitated extrusion based 3D printing for pharmaceuticals. European Journal of Pharmaceutical Sciences 152, 105430.
Duarte, A.R., Roy, C., Vega-González, A., Duarte, C.M., Subra-Paternault, P., 2007. Preparation of acetazolamide composite microparticles by supercritical anti-solvent techniques. Int J Pharm 332, 132-139.
Evonik, EUDRAGIT® functional polymers for sustained release.
Faitel'son, L.A., Alekseenko, A.I., 1977. Effect of filler on the viscosity and viscoelasticity of melts of low-density polyethylene. Communication 2. Polymer Mechanics 13, 118-122.
Fanous, M., Gold, S., Muller, S., Hirsch, S., Ogorka, J., Imanidis, G., 2020. Simplification of fused deposition modeling 3D-printing paradigm: Feasibility of 1-step direct powder printing for immediate release dosage form production. International Journal of Pharmaceutics 578, 119124.
Farrell, T.P.T., Jason; Friend, Barry ;Gulian, Scott 2010. Film coatings containing fine particle size detackifiers and substrates coated therewith
FDA, 2017. Q4B Evaluation and Recommendation of Pharmacopoeial Texts for Use in the ICH Regions: Annex 9(R1) Tablet Friability General Chapter Guidance for Industry
Glaessl, B., Siepmann, F., Tucker, I., Rades, T., J.Siepmann, 2010. Mathematical modeling of drug release from Eudragit RS-based delivery systems. Journal of Drug Delivery Science and Technology 20, 127-133.
Goyanes, A., Allahham, N., Trenfield, S.J., Stoyanov, E., Gaisford, S., Basit, A.W., 2019. Direct powder extrusion 3D printing: Fabrication of drug products using a novel single-step process. International Journal of Pharmaceutics 567, 118471.
Jelvehgari, M., Montazam, S.H., 2012. Comparison of microencapsulation by emulsion-solvent extraction/evaporation technique using derivatives cellulose and acrylate-methacrylate copolymer as carriers. Jundishapur J Nat Pharm Prod 7, 144-152.
Khaled, S., Burley, J., Alexander, M., Yang, J., Roberts, C., 2015a. 3D printing of five-in-one dose combination polypill with defined immediate and sustained release profiles. Journal of controlled release : official journal of the Controlled Release Society 217.

Khaled, S.A., Alexander, M.R., Irvine, D.J., Wildman, R.D., Wallace, M.J., Sharpe, S., Yoo, J., Roberts, C.J., 2018. Extrusion 3D Printing of Paracetamol Tablets from a Single Formulation with Tunable Release Profiles Through Control of Tablet Geometry. AAPS PharmSciTech 19, 3403-3413.
Khaled, S.A., Burley, J.C., Alexander, M.R., Roberts, C.J., 2014. Desktop 3D printing of controlled release pharmaceutical bilayer tablets. Int J Pharm 461, 105-111.
Khaled, S.A., Burley, J.C., Alexander, M.R., Yang, J., Roberts, C.J., 2015b. 3D printing of tablets containing multiple drugs with defined release profiles. Int J Pharm 494, 643-650.
Kollamaram, G., Croker, D.M., Walker, G.M., Goyanes, A., Basit, A.W., Gaisford, S., 2018. Low temperature fused deposition modeling (FDM) 3D printing of thermolabile drugs. Int J Pharm 545, 144-152.
Krause, J., Bogdahn, M., Schneider, F., Koziolek, M., Weitschies, W., 2019. Design and characterization of a novel 3D printed pressure-controlled drug delivery system. European Journal of Pharmaceutical Sciences 140, 105060.
Laila, S., Haque, T., Talukder, M., Ahmed, I., Islam, M., Rahman, H., 2009. Development of Glyceryl Monostearate Based Ciprofloxacin Hydrochloride Sustained Release Matrix Tablet: In vitro Study. Dhaka University Journal of Pharmaceutical Science 8.
Lehmann, K., 1986. In Wasser dispergierbare, hydrophile Acrylharze mit abgestufter Permeabilität für diffusionsgesteuerte Wirkstoffabgabe aus Arzneiformen,. Acta Pharm Technol, 146–152.
Lehmann, K., 1997. Chemistry and application properties of polymethacrylate coating system. Marcel Dekker, New York.
Li, P., Jia, H., Zhang, S., Yang, Y., Sun, H., Wang, H., Pan, W., Yin, F., Yang, X., 2019. Thermal Extrusion 3D Printing for the Fabrication of Puerarin Immediate-Release Tablets. AAPS PharmSciTech 21, 20.
Li, Q., Guan, X., Cui, M., Zhu, Z., Chen, K., Wen, H., Jia, D., Hou, J., Xu, W., Yang, X., Pan, W., 2018. Preparation and investigation of novel gastro-floating tablets with 3D extrusion-based printing. International Journal of Pharmaceutics 535, 325-332.
Melocchi, A., Parietti, F., Maroni, A., Foppoli, A., Gazzaniga, A., Zema, L., 2016. Hot-melt extruded filaments based on pharmaceutical grade polymers for 3D printing by fused deposition modeling. International Journal of Pharmaceutics 509, 255-263.
Okwuosa, T.C., Stefaniak, D., Arafat, B., Isreb, A., Wan, K.W., Alhnan, M.A., 2016. A Lower Temperature FDM 3D Printing for the Manufacture of Patient-Specific Immediate Release Tablets. Pharm Res 33, 2704-2712.
Peh, K.K., Wong, C.F., Yuen, K.H., 2000. Possible mechanism for drug retardation from glyceryl monostearate matrix system. Drug Dev Ind Pharm 26, 447-450.
Pereira, B.C., Isreb, A., Forbes, R.T., Dores, F., Habashy, R., Petit, J.B., Alhnan, M.A., Oga, E.F., 2019. 'Temporary Plasticiser': A novel solution to fabricate 3D printed patient-centred cardiovascular 'Polypill' architectures. Eur J Pharm Biopharm 135, 94-103.
Peri, D., Bogdansky, S., Allababidi, S., Shah, J.C., 1994. Development of an Implantable, Biodegradable, Controlled Drug Delivery System for Local Antibiotic Therapy. Drug Development and Industrial Pharmacy 20, 1341-1352.
Pietrzak, K., Isreb, A., Alhnan, M.A., 2015. A flexible-dose dispenser for immediate and extended release 3D printed tablets. Eur J Pharm Biopharm 96, 380-387.
Pravin, S., Sudhir, A., 2018. Integration of 3D printing with dosage forms: A new perspective for modern healthcare. Biomedicine & Pharmacotherapy 107, 146-154.
Qushawy, M., Prabahar, K., Abd-Alhaseeb, M., Swidan, S., Nasr, A., 2019. Preparation and Evaluation of Carbamazepine Solid Lipid Nanoparticle for Alleviating Seizure Activity in Pentylenetetrazole-Kindled Mice. Molecules 24, 3971.
Rajsharad, C.K., Shivaji 2005. Pva based film coating and film coating compositions
Rowe, R.S., PJ; Quinn, Marian E, 2009. Handbook of Pharmaceutical Excipients 6th ed. Pharmaceutical Press, London.
Siepmann, F., Siepmann, J., Walther, M., MacRae, R.J., Bodmeier, R., 2008. Polymer blends for controlled release coatings. J Control Release 125, 1-15.

Skowyra, J., Pietrzak, K., Alhnan, M.A., 2015. Fabrication of extended-release patient-tailored prednisolone tablets via fused deposition modelling (FDM) 3D printing. Eur J Pharm Sci 68, 11-17.
Steward, P.A., Hearn, J., Wilkinson, M.C., 1995. Studies on permeation through polymer latex films, I. Films containing no or only low levels of additives. Polymer International 38, 1-12.
Tagami, T., Ando, M., Nagata, N., Goto, E., Yoshimura, N., Takeuchi, T., Noda, T., Ozeki, T., 2019. Fabrication of Naftopidil-Loaded Tablets Using a Semisolid Extrusion-Type 3D Printer and the Characteristics of the Printed Hydrogel and Resulting Tablets. Journal of Pharmaceutical Sciences 108, 907-913.
Wagner, K., McGinity, J., 2002. Influence of chloride ion exchange on the permeability and drug release of Eudragit RS 30 D films. J Control Release 82, 385-397.
Yan, T.T., Lv, Z.F., Tian, P., Lin, M.M., Lin, W., Huang, S.Y., Chen, Y.Z., 2020. Semi-solid extrusion 3D printing ODFs: an individual drug delivery system for small scale pharmacy. Drug Dev Ind Pharm 46, 531-538.
Yang, Y., Wang, X., Lin, X., Xie, L., Ivone, R., Shen, J., Yang, G., 2020. A tunable extruded 3D printing platform using thermo-sensitive pastes. International Journal of Pharmaceutics 583, 119360.
Zhu, Y., Shah, N.H., Malick, A.W., Infeld, M.H., McGinity, J.W., 2004. Influence of a lipophilic thermal lubricant on the processing conditions and drug release properties of chlorpheniramine maleate tablets prepared by hot-melt extrusion. Journal of Drug Delivery Science and Technology 14, 313-318.

List of figures

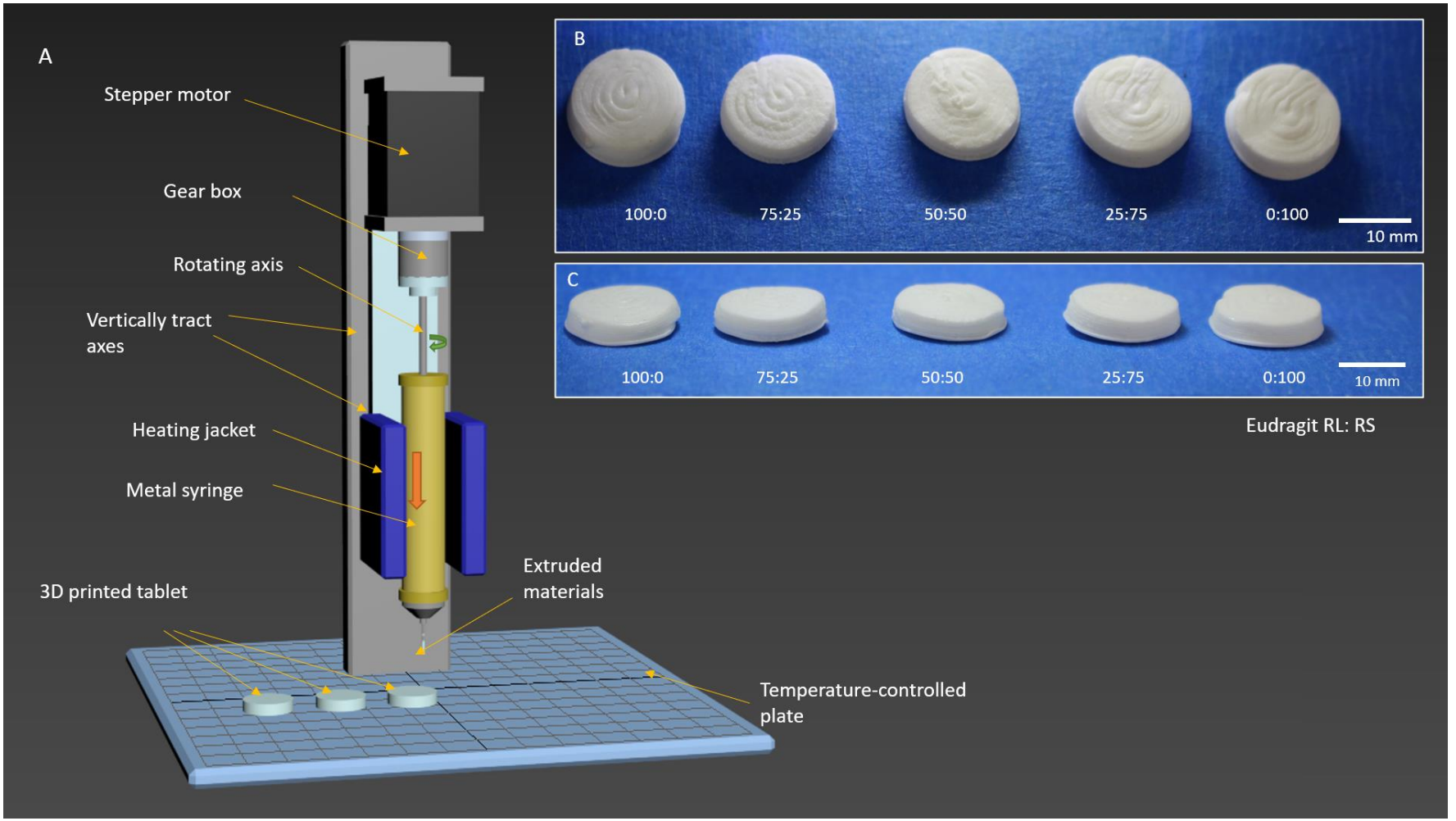

Fig. 1. (A) Set-up for semi-solid extrusion 3D printing. (a) The printer is equipped with a metal syringe surrounded by temperature-controlled heating jacket. The syringe is fitted with a luer-lock stainless steel needle (G18), (b) The pharmaceutical ink (compressed powder) is added. The ink is then extruded by a piston pushed by computer-controlled stepper motor equipped with gear to produce (c) 3D printed tablet. (**B**) Top and (**C**) side photographs of 3D printed tablets based on Eudragit RL: RS: 100:0, 75:25, 50:50, 25:75 and 0:100.

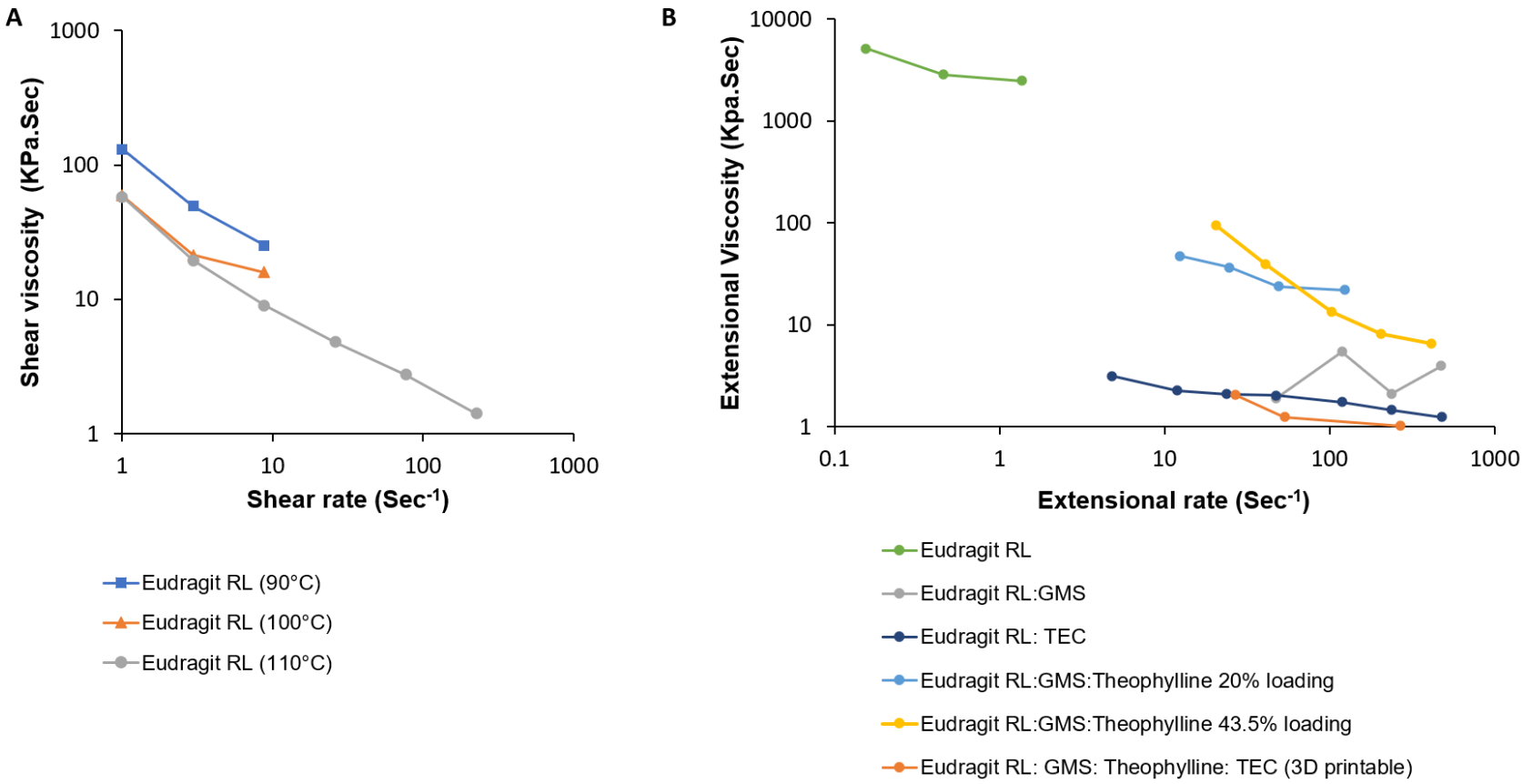

Fig. 2 (A) Shear viscosity of Eudragit RL 100 at temperature range of 90-110°C, **(B)** Extensional viscosity data of mixtures.

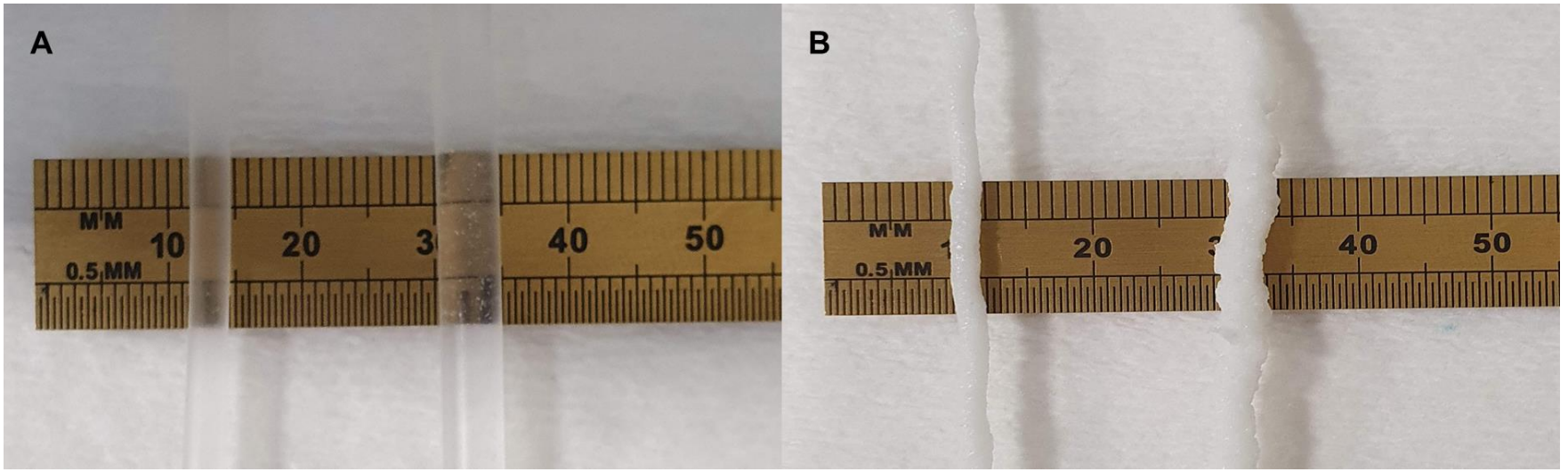

Fig. 3 (A) Eudragit RL extruded at 110°C using a long die (left, d=3.5mm), and an orifice die (right, d=5mm) **(B)** Eudragit RL formulation extruded at 90°C using long die (left, d=1.5mm), and an orifice die (right, d=4mm).

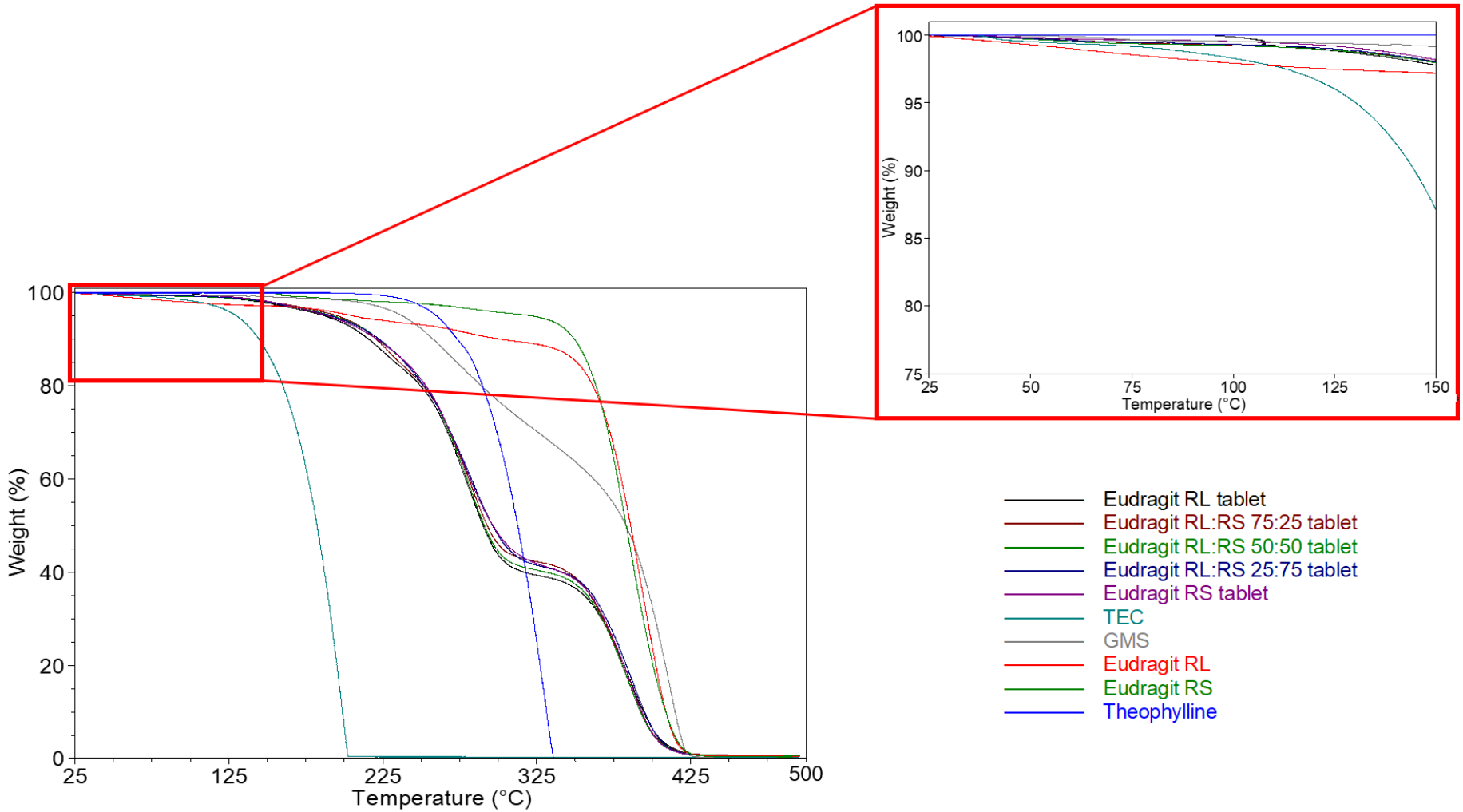

Fig. 4 TGA thermal degradation profiles of raw theophylline, Eudragit RL, Eudragit RS, TEC, GMS, and 3D printed tablets based on Eudragit RL: RS: 100:0, 75:25, 50:50, 25:75 and 0:100.

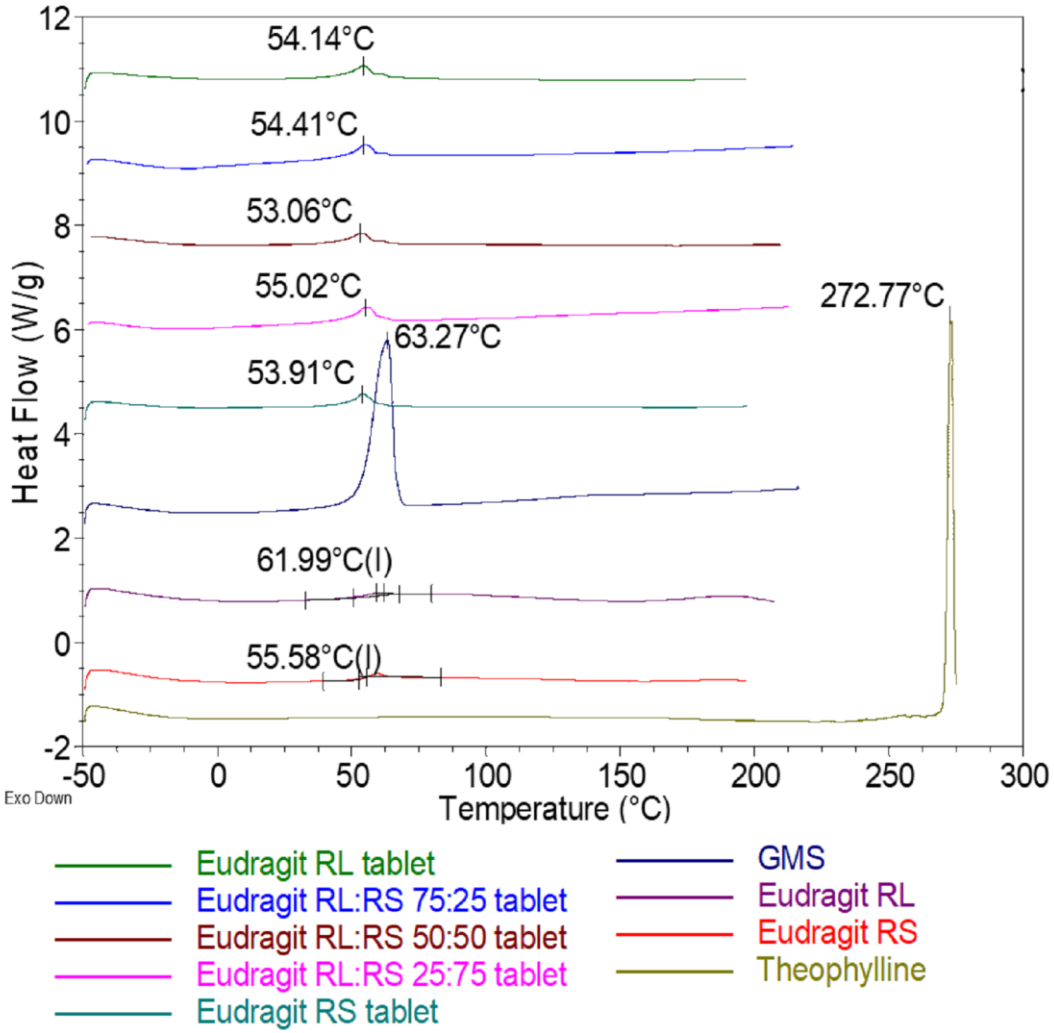

Fig. 5 DSC thermograph of raw theophylline, Eudragit RL, Eudragit RS, TEC, GMS, and 3D printed tablets based on Eudragit RL: RS: 100:0, 75:25, 50:50, 25:75 and 0:100.

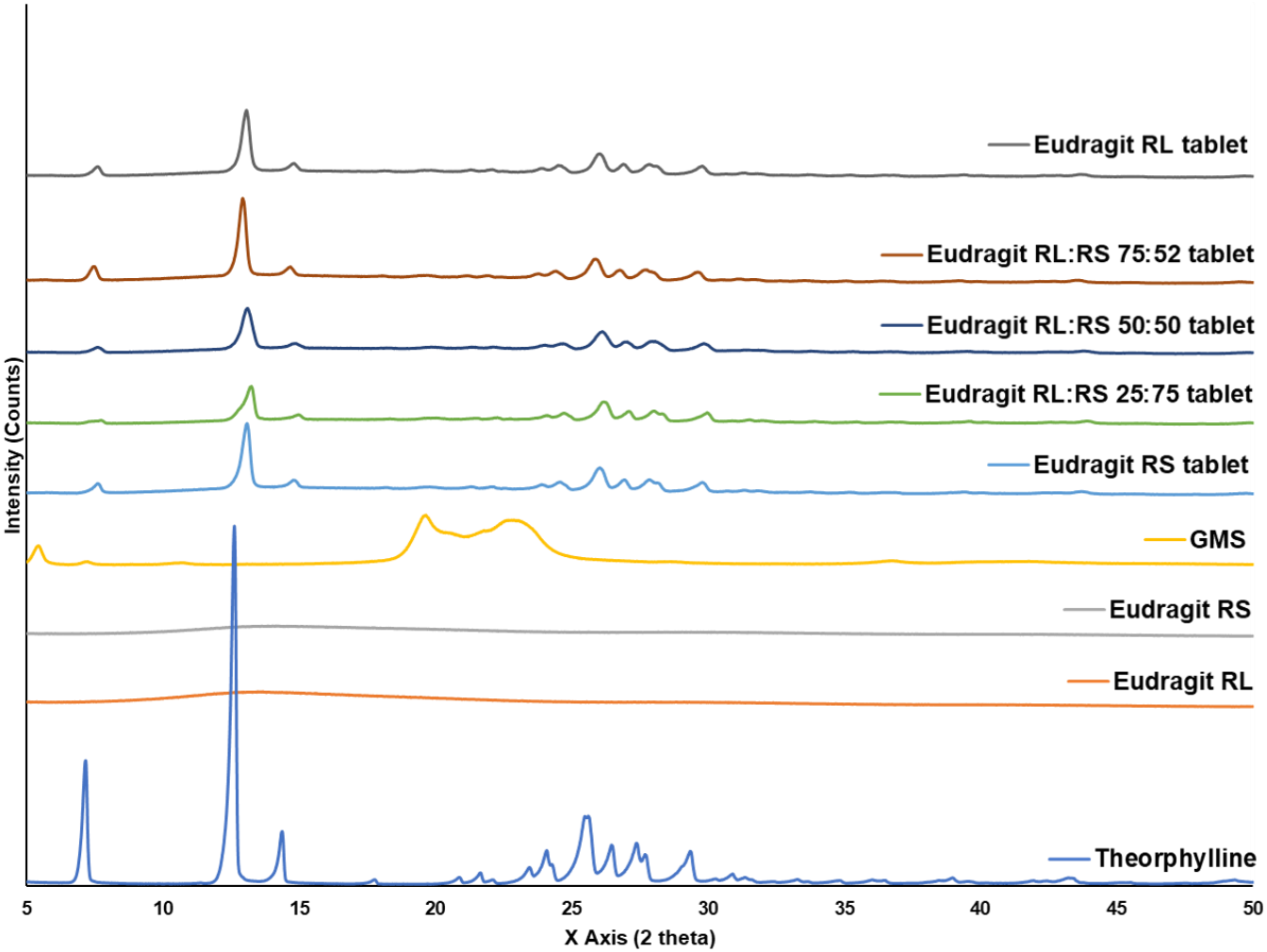

Fig. 6 XRPD of raw theophylline, Eudragit RL, Eudragit RS, TEC, GMS, and 3D printed tablets based on Eudragit RL: RS: 100:0, 75:25, 50:50, 25:75 and 0:100.

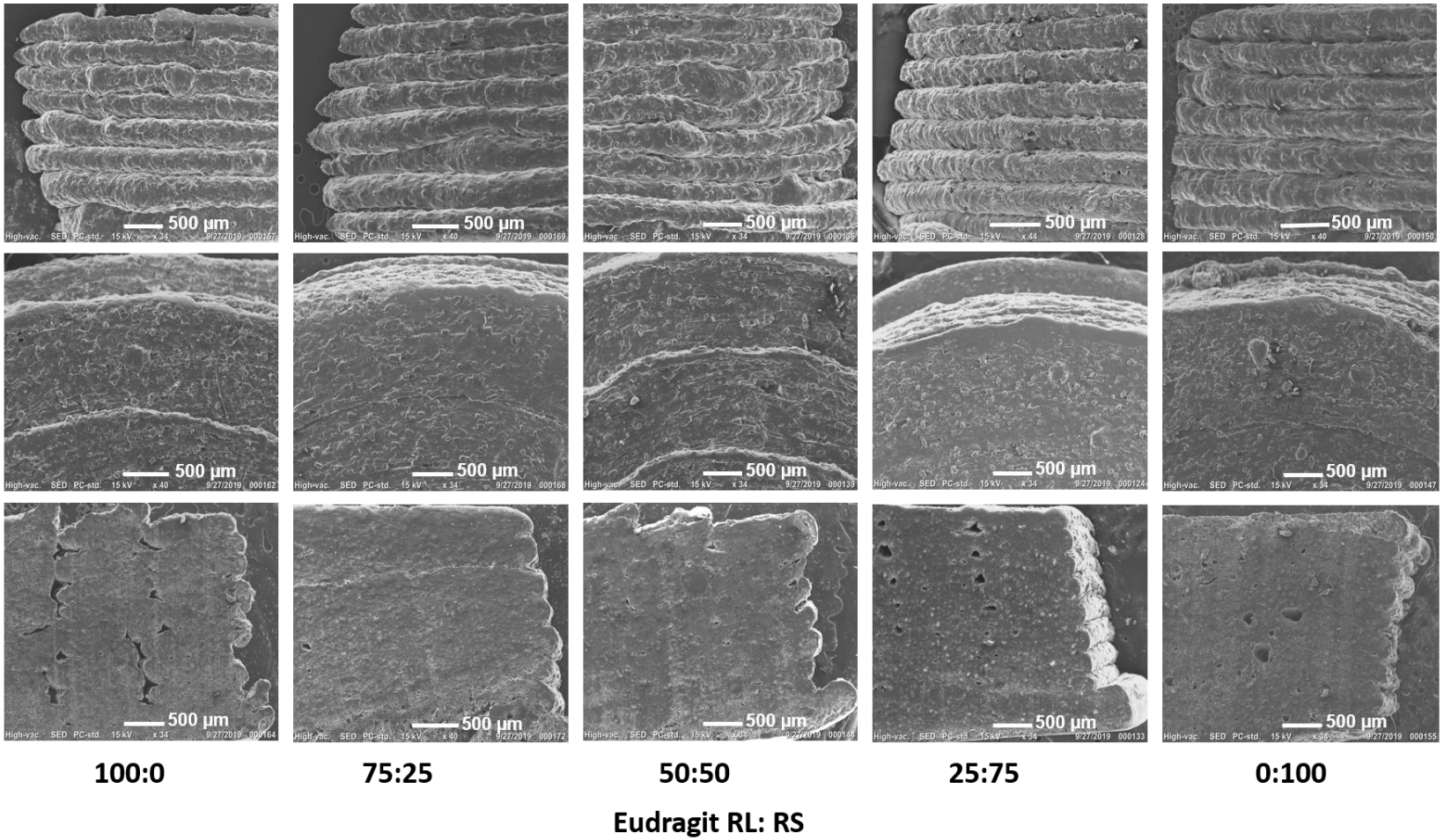

Fig. 7 SEM images of side-view (A1,B1, C1, D1 and E1) , top view (A2,B2, C2, D2 and E2) and cross sections of 3D printed tablets based on Eudragit RL: RS: 100:0, 75:25, 50:50, 25:75 and 0:100 respectively.

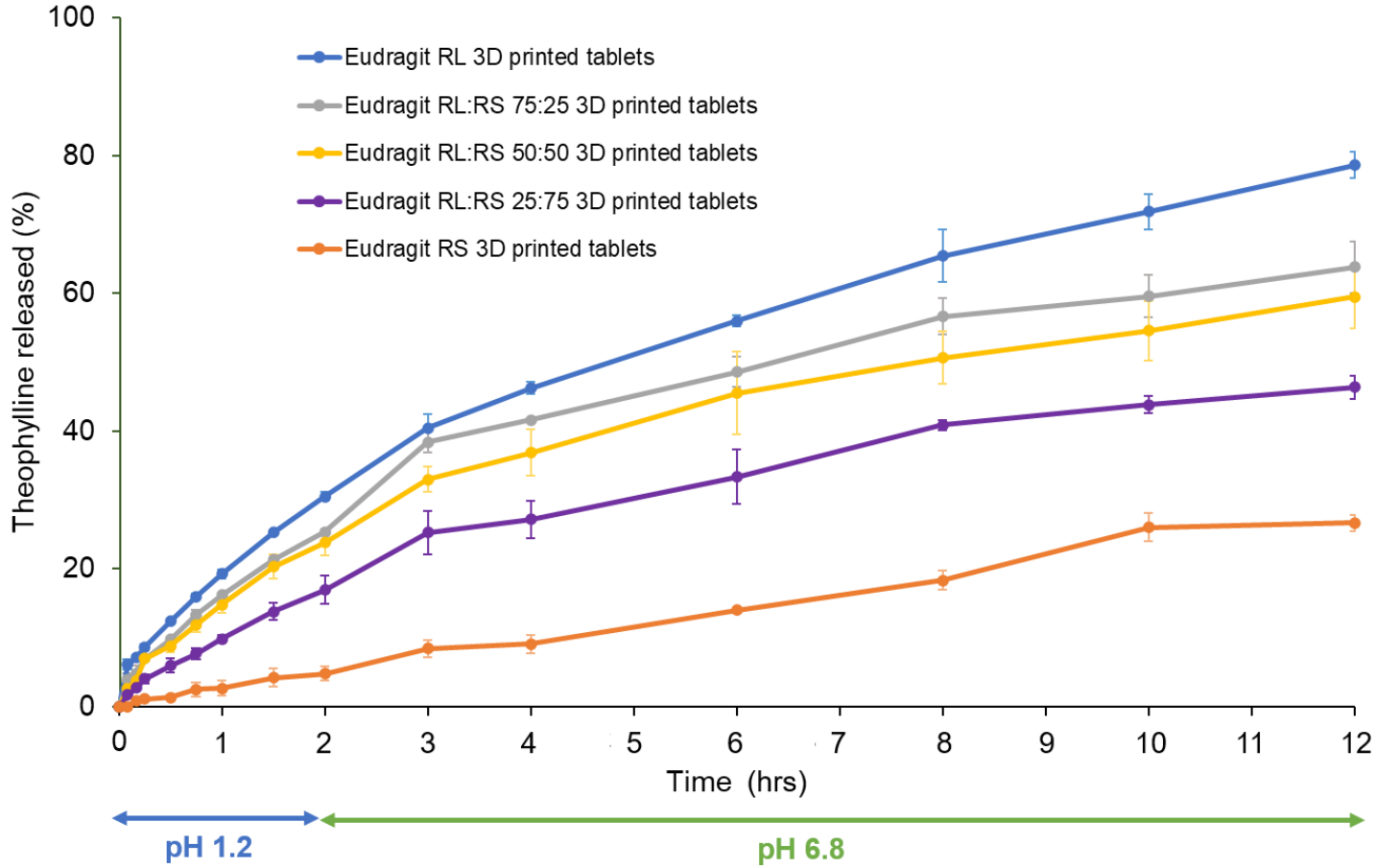

Fig. 8 *In vitro* release of theophylline from 3D printed tablets based on Eudragit RL: RS: 100:0, 75:25, 50:50, 25:75 and 0:100 using pH-change USPII dissolution test (pH 1.2 for 2 hours followed by pH 6.8 for 10 hours, n= 3, ±SD).